Bull. Chem. Soc. Jpn., *58, 1543—1550 (1985)*

Fe K-Edge XANES and EXAFS of the X-Ray Absorption Spectra of $FeCl_3$ Aqueous Solutions.
A Structural Study of the Solute, Iron(III) Chloro Complexes

Kiyotaka Asakura, Masaharu Nomura,† and Haruo Kuroda*
Department of Chemistry and Research Center for Spectrochemistry, Faculty of Science, The University of Tokyo, Hongo, Bunkyo-ku, Tokyo 113
(Received September 3, 1984)

The Fe K-edge spectra were measured on $FeCl_3$ aqueous solutions by use of synchrotron radiation to reveal the solute structure from the analysis of Fe K-edge EXAFS and XANES. It is concluded that the solute exists mainly as $[Fe(H_2O)_6]^{3+}$ but partially as $[FeCl(H_2O)_5]^{3+}$ at $FeCl_3$ concentration of 0.1—1 mol dm^{-3}, and it exsits mainly as $[FeCl_2(H_2O)_4]^+$ at the concentration of 3—4 mol dm^{-3}. In the diliquescent product of $FeCl_3$, about a half of the solute is in the state of $[FeCl_4]^-$ and the remaining half is likely to be in the state of $[FeCl_2(H_2O)_4]^+$. No indication was found for the dimer formation of $FeCl_3$ even in the deliquescent product.

The structures of the iron(III) chloro complexes which are formed in the aqueous solution of $FeCl_3$, have been extensively investigated by means of X-ray diffraction.[1—10] But the conclusions given by different authors are still mutually conflicting in several respects. Recently, Magini *et al.* concluded that the dominant solute species existing in an aqueous solution of $FeCl_3$ at the concentration of about 4 mol dm^{-3} was octahedral chloro complexes.[5,10] On the other hand, Wertz *et al.* reported that the octahedral aqua complex $[Fe(H_2O)_6]^{3+}$ was dominant in the solution of the same concentration, which was freshly prepared from $FeCl_3\cdot6H_2O$, but octahedral chloro complexes $[FeCl_x(H_2O)_{6-x}]$ were gradually formed to have an average composition $[FeCl_{1.4}(H_2O)_{4.6}]$ after aging the solution for 14 months, whereas the tetrahedral chloro complexes were dominant when the solution was prepared from anhydrous $FeCl_3$.[7,8] From the examination of the X-ray diffraction pattern of the melt of $FeCl_3\cdot6H_2O$, Magini *et al.* claimed that the dimer of $FeCl_3$ was partially formed in this melt.[6] Wertz *et al.* also assumed without any direct experimental evidence, that the dimeric species Fe_2Cl_6 should exist also in a concentrated aqueous solution of about 4 mol dm^{-3} prepared from anhydrous $FeCl_3$.[7]

There could be several different kinds of the chloro complex coexisting in the $FeCl_3$ solution and the dominant species should vary depending on the solute concentration, but little is known about their equilibrium.[5] It is desirable to study over a wide range of the solute concentration from this point of view. But the X-ray diffraction studies hitherto reported were done only on the $FeCl_3$ solutions of a relatively high concentration, mostly above 1 mol dm^{-3}, because X-ray diffraction data inevitably contain a large contribution of the diffraction by the solvent. In this respect, it is of great interest to use extended X-ray absorption fine structure (EXAFS) and X-ray absorption near edge structure (XANES), since one can obtain from the analysis of EXAFS and XANES of Fe K-edge spectrum the information on the local structure surrounding Fe atom without being greatly disturbed by the presence of solvent even in the case of a considerably dilute solution.[11] We have already used this technique successfully in the structural studies on the systems involving Fe–Cl bond such as anhydrous $FeCl_3$[12] and $FeCl_3$-doped polyacetylene.[13]

In the present study, we measured Fe K-edge EXAFS and XANES in the X-ray absorption spectra of $FeCl_3$ aqueous solutions to derive the structural information on the solute.

Experimental

Preliminary experiments of X-ray absorption spectra (XAS) were carried out by use of the in-laboratory EXAFS spectrometer which was described elsewhere,[14] but final XAS data were obtained by use of synchrotron radiation employing the EXAFS facilities at BL-10B of the Photon Factory in the National Laboratory for High-Energy Physics (KEK-PF). The details of this experimental setup have been described elsewhere.[15] In the present study, a Si(311) channel-cut crystal was used to monochromatize X-rays from 2.5 GeV electron storage ring. The sample cell used in the XAS measurement of a liquid sample had two hard polypropylene windows to pass X-rays. The separation between the two windows was variable by changing the spacer between the windows. We set the sample thickness so as to keep the absolute absorbance at Fe K-edge below 3.0 in all cases. All XAS measurements were carried out at room temperature.

The sample solutions investigated in the present study are listed in Table 1, together with their abbreviated symbols, where the number stands for the concentration in mol dm^{-3} and the characters N and A stand for the neutral and acidified cases, respectively. Each solution was prepared by dissolving an appropriate amount of $FeCl_3\cdot6H_2O$ (reagent grade) into distilled water. We used nitric acid to acidify the solution except in the sample which is

---

† Present address: Photon Factory, Natinal Laboratory for High Energy Physics, Oho-machi, Tsukuba-gun, Ibaraki 305.

Table 1. Compositions of the solutions

Symbols of Samples	Fe^{3+} / mol dm^{-3}	$[HNO_3]$ / $[Fe^{3+}]$	$[HCl]$ / $[Fe^{3+}]$
4N	4.3		
3N	3.0		
0.7N	0.74		
0.1N	0.14		
3A	3.0	1	
0.5A	0.50	1	
Cl3A	3.1		1
DP	Deliquescent product of anhydrous $FeCl_3$		

denoted as Cl3A where HCl was used to see the effect of Cl^- ion, the ratio [acid]/[$FeCl_3$] being unity in all acidified samples. The deliquescent product of anhydrous $FeCl_3$(DP in Table 1) was taken up as the most concentrated non-acidified solution of $FeCl_3$.

We also measured the UV-visible absorption spectra of the sample solutions in order to characterize the solute state by comparing them with the reported data.[16–18] In the measurement of UV-visible absorption spectrum, perchloric acid was used to acidify the solutions instead of nitric acid, because NO_3^- has a strong absorption band at 220 nm.

Results

UV-visible absorption spectrum is known to be useful to characterize the coordination state of iron(III) complex. The absorption spectrum of a nitromethane solution of $[N(C_2H_5)_4]\,[FeCl_4]$ and that of an aqueous solution of $Fe(ClO_4)_3 \cdot 6H_2O$ are shown in Fig. 1. The former is a typical case where the solute exists exclusively in the form of $[FeCl_4]^-$. The strong peaks at 317 and 365 nm and the weak peaks at 446, 532, 606, 685, and 728 nm in its absorption spectrum are the ones characteristic of $[FeCl_4]^-$.[19] In the aqueous solution of $Fe(ClO_4)_3 \cdot 6H_2O$, the peaks at 240 and 330 nm and the shoulder at 440 nm are the structure characteristic of $[Fe(H_2O)_6]^{3+}$ and its hydrolysis products.[20] We denote the species existing in this case as $[Fe(H_2O)_6]^{3+}$ for convenience, although it could be partially in the state of the hydrolysis product. The UV-visible absorption spectra of non-acidified aqueous solutions of $FeCl_3$ are shown in Fig. 2. According to the general features of the observed spectra, we can classify the solutions into the following three groups; the solutions where $FeCl_3$ concentration is less than 1 mol dm^{-3} (Group 1), the solutions with the concentration of 3—4 mol dm^{-3} (Group 2) and the very concentrated solutions such as DP (Group 3). The absorption spectra of the solutions of Group 1 exhibit strong peaks at 220 and 335 nm, and resemble the spectrum of $[Fe(H_2O)_6]^{3+}$ except for a small difference as regards the positions and relative intensities of absorption maxima. This type of spectrum has been attributed to the octahedral chloro complexes such as $[FeCl(H_2O)_5]^{2+}$ and/or $[FeCl_2(H_2O)_4]^+$.[16–18] On the other hand, the absorption spectrum of DP (a solution of Group 3) exhibits the features characteristic of $[FeCl_4]^-$, suggesting that $[FeCl_4]^-$ is the dominant species in this case. The spectra of

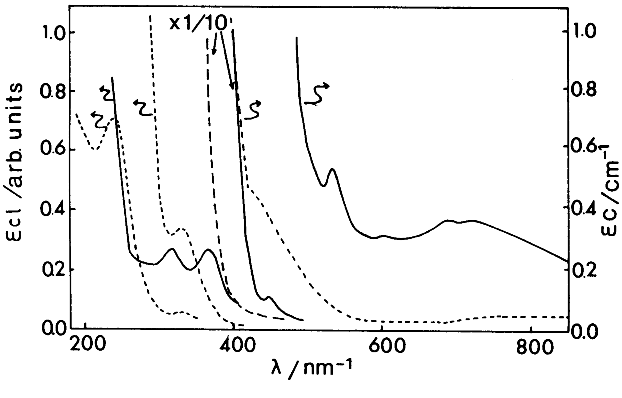

Fig. 1. UV-visible absorption spectra of the nitromethane solution of $[N(C_2H_5)_4][FeCl_4]$ (solid line) and the aqueous solution of $Fe(ClO_4)_3 \cdot 6H_2O$ (broken line).

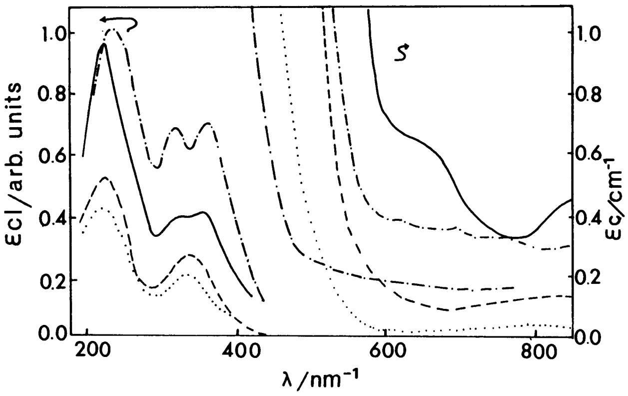

Fig. 2. UV-visible absorption spectra of non-acidified aqueous solutions of $FeCl_3$. —·—: DP, ——: 4N, — —: 1N, ······: 0.2N.

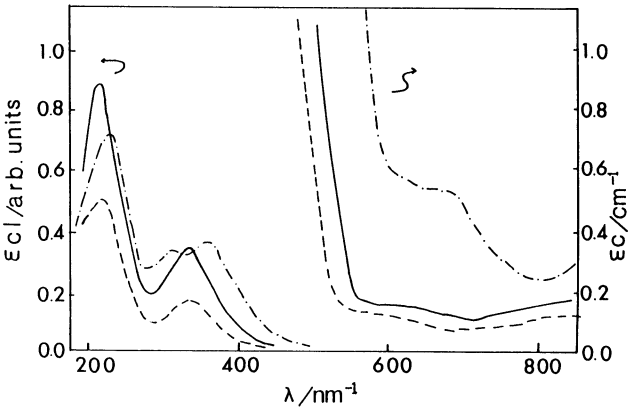

Fig. 3. UV-visible absorption spectra of acidified aqueous solutions of $FeCl_3$. —·—: 3A, ——: 1A, — —: 0.5A.

the solutions of Group 2 show the features in-between the above-mentioned two cases. This seems to be due to the co-existence of the octahedral and tetrahedral complexes. Figure 3 shows the spectra of the solutions acidified with perchloric acid. No remarkable change can be found in the spectrum on acidifying the solution.

Figure 4 shows the Fe K-edge region of the X-ray absorption spectra of the crystalline powders of $Fe(NO_3)_3 \cdot 9H_2O$, $FeCl_3 \cdot 6H_2O$, and $[N(C_2H_5)_4][FeCl_4]$. In these compounds, the local structure around Fe atom can be described as $[Fe(H_2O)_6]^{3+}$, *trans*- $[FeCl_2(H_2O)_4]^+$, and $[FeCl_4]^-$, respectively. Since XANES is determined by the local structure surrounding the X-ray absorbing atom, the spectra shown here can be taken respectively as those characteristic of the above-mentioned three kinds of iron(III) complex. All three spectra show a pre-edge structure which is attributable to the 1s–3d transition, but its shape and intensity are different between octahedral complexes and a tetrahedral one. In the cases of $[Fe(H_2O)_6]^{3+}$ and $[FeCl_2(H_2O)_4]^+$, both of which are octahedral complexes, the 1s–3d transition splits into two weak peaks, whereas it gives a relatively strong sharp peak in the case of the tetrahedral complex $[FeCl_4]^-$. Difference can be found also in the region above the absorption edge. The spectrum of $[Fe(H_2O)_6]^{3+}$ exhibits a considerably sharp peak just above the absorption edge, which is accompanied by a weak shoulder structure, the spectrum of $[FeCl_2(H_2O)_4]^+$ shows two broad absorption maxima around the absorption edge, and the spectrum of $[FeCl_4]^-$ exhibits three relatively sharp peaks followed by a broad structure.

XANES regions of the X-ray absorption spectra of the non-acidified solutions are shown in Fig. 5. The spectra shown here can be classified into three types. The first is the case observed for relatively dilute solutions where $FeCl_3$ concentration is less than 1 mol dm^{-3}. In this case, the spectrum exhibits weak 1s–3d double peaks in the pre-edge region and a relatively sharp peak just above the absorption edge. The second is the case observed for the solutions of the concentration range of 3—4 mol dm^{-3}, where the spectra again show weak double pre-edge peaks like in the first case, but the maximum just above the absorption edge splits into two peaks. The third is the case observed for a very concentrated solution like DP. In this case, the spectrum shows a sharp pre-edge 1s–3d peak and a shoulder structure and two peaks around the absorption edge. This classification of non-acidified solutions from XANES corresponds to the one which we have done from UV-visible absorption spectroscopy. The appearance of weak double pre-edge peaks associated with 1s–3d transition is characteristic of iron(III) octahedral complex as we have mentioned. The spectrum of the first type,observed for the relatively dilute solutions (the solutions of Group 1), resembles the spectrum of $[Fe(H_2O)_6]^{3+}$, but the spectral shape above the absorption edge is a little different from the latter. Seemingly the difference is due to the coexistence of the octahedral chloro complex. The general shape of the

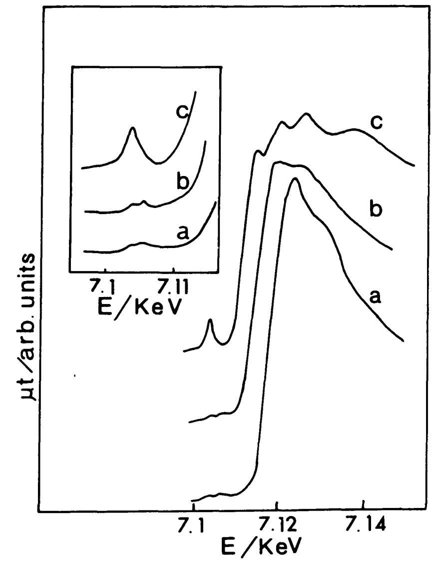

Fig. 4. Fe K-edge XANES spectra of reference compounds. (a): $Fe(NO_3)_3 \cdot 9H_2O$, (b): $FeCl_3 \cdot 6H_2O$, (c): $[N(C_2H_5)_4][FeCl_4]$. The pre-edge region is shown in the inset with an expanded scale.

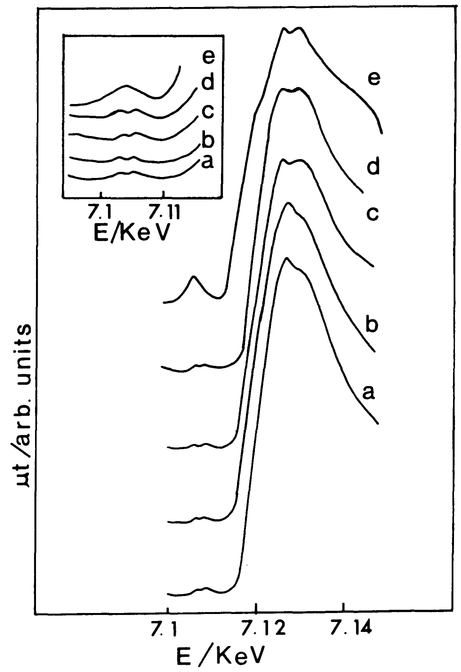

Fig. 5. Fe K-edge XANES spectra of non-acidified solutions of $FeCl_3$. (a): 0.1N, (b): 0.7N, (c): 3N, (d): 4N, (e): DP. The pre-edge region is shown in the inset with an expanded scale.

spectrum of the second type, observed for the 3—4 mol dm^{-3} solutions (the solutions of Group 2), corresponds to the spectrum of [$FeCl_2(H_2O)_4$]$^+$, indicating that the solute exists predominantly in the state of the octahedral chloro complex, but there are relatively sharp structrures above the absorption edge, which look like the structures due to [$FeCl_4$]$^-$ coexisting in the solution. The spectrum of DP exhibits a sharp single pre-edge 1s-3d peak and relatively sharp structures above the absorption edge, both of which are characteristic of the tetrahedral complex [$FeCl_4$]$^-$. However, the intensity of the pre-edge peak relative to the Fe K-edge jump is significantly smaller as compared with the spectrum of [$N(C_2H_5)_4$] [$FeCl_4$]. This fact indicates that the solution contains not only [$FeCl_4$]$^-$, but also octahedral complexes. The above-mentioned conclusions derived from XANES are consistent with those from UV-visible absorption spectroscopy. From the intensity of the pre-edge peak relative to the edge-jump, we approximately estimate the fraction of [$FeCl_4$]$^-$ ion among the total amount of the solute to be about 50%.[21]

Figure 6 shows the XANES spectra of the acidified solutions. Their spectral shapes are almost the same as those of the non-acidified solutions. Wertz *et al.* suggested that [$FeCl_4$]$^-$ comes to be the prominent species when the solution is acidified with hydrochloric acid.[9] However, little difference was observed among the spectra of C13A, 3A, and 3N. This means that the main species are not significantly different among these solutions and that [$FeCl_4$]$^-$ is not predominant in C13A.

The EXAFS oscillation $\chi(k)$ was extracted from an observed XAS spectrum by the following way. The smoothly varying component $\mu_s(\lambda)$ was estimated by fitting the observed spectrum using the cubic spline technique.[11] We estimated the absorbance for the free atom, $\mu_0(\lambda)$, in the region of 50—60eV from the edge by subtracting the background μ_b from μ_s. The background μ_b was determined by a smooth extrapolation from the pre-edge region by use of Victoreen's equation.

$$\mu_b(\lambda) = C\lambda^3 + D\lambda^4 \qquad (1)$$

The μ_0 value in other region was estimated by assuming that its wavelength dependence was describable with the Victreen's equation, the parameters of which were taken from the literature.[22] The photon energy E was converted to the photoelectron wave number k by Eq. 2.

$$k = \sqrt{2m(E-E_0)}/\hbar \qquad (2)$$

where E_0 is the ionization threshold. Then the EXAFS oscillation $\chi(k)$ was calculated by using Eq. 3.

$$\chi(k) = (\mu-\mu_s)/\mu_0 \qquad (3)$$

The Fourier transforms of $k^3\cdot\chi(k)$ over the region of k=4.0—12.0 Å^{-1} are shown in Figs. 7—9. Both for non-acidified and acidified cases, the main peak of Fourier transform is at 1.60—1.61 Å when the solute concentration is less than 1 mol dm^{-3} (the

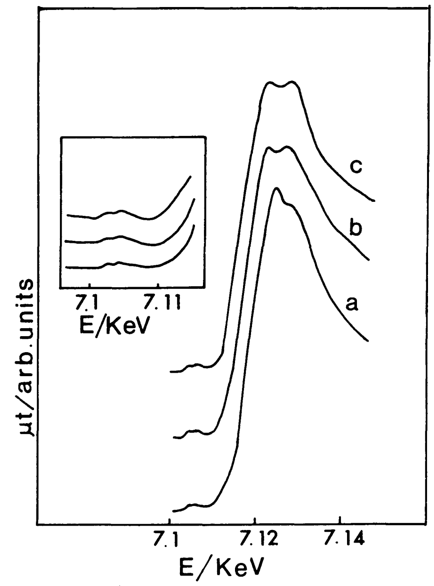

Fig. 6. Fe K-edge XANES spectra of acidified solutions of $FeCl_3$. (a): 0.5A, (b): 3A, (c): C13A. The pre-edge region is shown in the inset with an expanded scale.

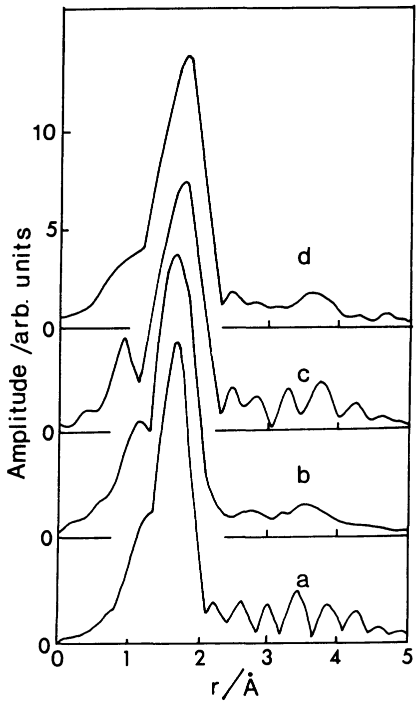

Fig. 7. Fourier transfeorms of $k^3\cdot\chi(k)$ for non-acidified aqueous solutions of $FeCl_3$. (a): 0.1N, (b): 0.7N, (c): 3N, (d): 4N.

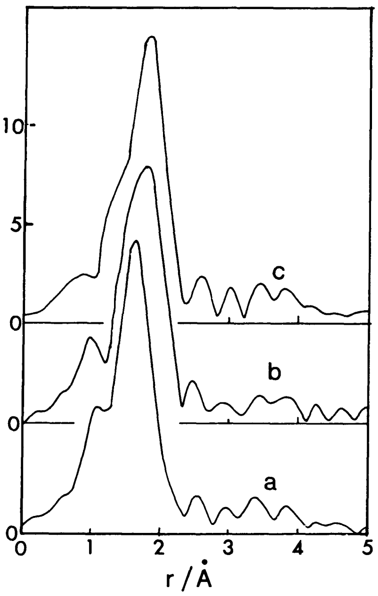

Fig. 8. Fourier transforms of $k^3 \cdot \chi(k)$ for acidified aqueous solutions of $FeCl_3$. (a): 0.5A, (b): 3A, (c): Cl3A.

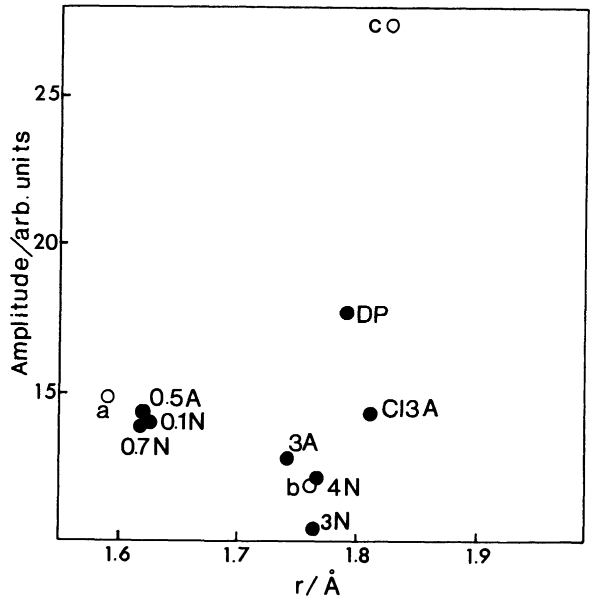

Fig. 10. Plots of the amplitude of the main peak of Fourier transform against the peak position.
(a): $Fe(NO_3)_3 \cdot 9H_2O$, (b): $FeCl_3 \cdot 6H_2O$, (c): $[N(C_2H_5)_4][FeCl_4]$. Refer to Table 1 for abbreviated symbols of the solutions.

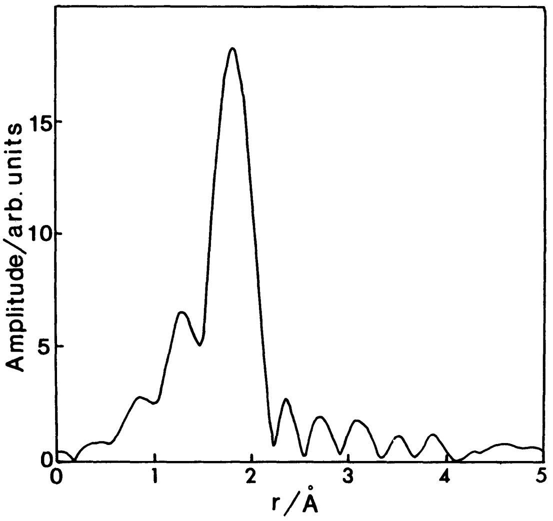

Fig. 9. Fourier transform of $k^3 \cdot \chi(k)$ for DP.

solutions of Group 1), but the corresponding peak shifts to 1.76 Å in the case of DP. The solutions of the Group 2 show the corresponding peak at a position in-between these two cases. The above-mentioned main peak of Fourier transform is attributable to Fe–Cl and/or Fe–O(H_2O). Since Fe–Cl distance is longer than Fe–O distance, the shift of the main peak is associated with the increase of the number of Cl atoms coordinating to Fe atom. The peak amplitude should be also dependent on the Cl/O ratio surrounding Fe atom. In Fig.10, we plotted the amplitude of the main peak of Fourier transform against the peak position. The position of the point in this plot could be a good criterion of the average state of the solute.[23] Note that the points for the solutions 0.1N, 0.7N, and 0.5A (Group 1) are nearly at the same position, whereas the points for much concentrated solutions fall in a quite different area. We have also shown the points obtained for the reference materials in which the local structures surrounding Fe atom are $[Fe(H_2O)_6]^{3+}$, $[FeCl_2(H_2O)_4]^+$ and $[FeCl_4]^-$, respectively. We can see that the point for $[Fe(H_2O)_6]^{3+}$ is located at the position shifted a little to the left from the points for the $FeCl_3$ solutions of Group 1, and the point for $[FeCl_2(H_2O)_4]^+$ is in the area where the points for much concentrated $FeCl_3$ solutions are located. This fact again indicates that the solute is in the state of $[Fe(H_2O)_6]^{3+}$ along with chloro complexes in the solutions of Group 1, while it is mainly in the states of $[FeCl_2(H_2O)_4]^+$ and other chloro complexes in much concentrated solutions. Note that the point for DP is significantly separated from the point for $[FeCl_4]^-$. This fact again indicates that the solute is not entirely in the state of $[FeCl_4]^-$ in DP as we have concluded from XANES.

Performing the inverse Fourier transformation over the region of the main peak (r=1.0–2.2 Å) of each Fourier transform, we carried out further analysis of EXAFS oscillation by means of the nonlinear least square curve-fitting method, using the Eq.4.

$$k^3 \cdot \chi(k) = \sum_j k^2 S_j(k)(N_j/r_j^2)F_j(k) \times \exp(-2\sigma_j^2 k^2) \sin(2kr_j + \phi_j(k)) \tag{4}$$

TABLE 2. RESULTS OF THE CURVE-FITTING ANALYSIS OF THE EXAFS DATA OF THE REFERENCE COMPOUNDS

Sample	Coordination number		Distance (r/Å)*		S**
	Cl	O	Fe-Cl	Fe-O	
$Fe(NO_3)_3 \cdot 9H_2O$	0	6		1.90 (2) $[1.99]^{a)}$	0.43
$FeCl_3 \cdot 6H_2O$	2	4	2.30 (3) $[2.30]^{b)}$	2.06 (3) $[2.07]^{b)}$	0.40
$[N(C_2H_5)_4][FeCl_4]$	4	0	2.19 (2) $[2.19]^{c)}$		0.53
$(NH_4)_2[FeCl_5(H_2O)]$	5	1	2.34 (3) $[2.38]^{d)}$	2.05 (3) $[2.08]^{d)}$	0.43
$[Co(NH_3)_6][FeCl_6]$	6	0	2.37 (2) $[2.39]^{e)}$		0.50

* The interatomic distances determined by crystal structure analysis are given in brackets; (a) from Ref. 30, (b) from Ref. 31, (c) from Ref. 32, (d) from Ref. 33, (e) from Ref. 34. ** The inaccuracy of these S values was found to be 20—30%.

where N_j is the coordination number of the j-th shell at the distance r_j from the X-ray absorbing atom, $F_j(k)$ the back-scattering amplitude for the photoelectron wave number k, $\phi_j(k)$ the phase shift, σ_j the Debye-Waller factor of the atoms in the j-th shell. $S_j(k)$ is the amplitude reduction factor, which was assumed to be independent of k in the present study.[24]

The theoretical functions given in the literature were used for $F_j(k)$ and $\phi_j(k)$ in Eq. 4.[25] The validity of the assumed back-scattering amplitude and phase shift founctions were checked by carrying out the analysis of the EXAFS of the reference samples. As shown in Table 2, the results from EXAFS showed a satisfactory agreement with the crystallographic data.

In general, the amplitude reduction factor S_j should be different for different kinds of atom. But we assumed it to be the same value for the nearest neighbor Cl and O atoms.[26] We took this approximation in order to avoid the nonlinear least square analysis converging to the odd minimum points.

In the final refinement stage, we assumed the sum of the coordination numbers of Cl and O to be 6 for all solutions except for DP, where the best fit between the observed and calculated EXAFS oscillations was attained when the coordination numbers of Cl and O were assumed to be 3 and 2, respectively. The above-mentioned assumption is based on the conclusions derived from XANES and UV-visible absorption spectra, which show that the main species are octahedral complexes in all solutions except DP. The final results of curve-fitting analysis are summarized in Table 3. The average Fe–O distance obtained in the present study was 2.0 Å, which is close to the value reported by Magini *et al.*[6] The Fe–Cl distances were found to be 2.26—2.35 Å for the solutions of Group 1 and Group 2. This value corresponds to the distance which is usually found for the octahedral chloro complexes in the crystals of iron(III) compounds: The distance is known to be 2.30 Å in $FeCl_3 \cdot 6H_2O$,[27] 2.36 Å in $FeSbCl_8 \cdot 8H_2O$[28] and 2.368 Å in FeOCl.[29] In the solutions of Group 1, the best result in the curve-fitting analysis was attained only when the contribution of Cl atoms was taken into account. Probably this means that a fraction of the solute is in the form of octahedral chloro complexes even in the relatively dilute solutions. The coordination numbers obtained for the solutions of Group 2, well correspond to $[FeCl_2(H_2O)_4]^+$. Possibly this is the main solute species in these solutions. The Fe–Cl distance found for DP is 2.22 Å, which is shorter than the Fe–Cl distances found for more dilute solutions. This Fe–Cl distance is close to the value expected for the tetrahedral complex $[FeCl_4]^-$, but the best fit was not attainable between the calculated and observed EXAFS oscillations when the contribution of O atoms was neglected. As we have already mentioned, the coordination numbers for the best fit are 3 and 2 for Cl and O, respectively. These average coordination numbers imply that the octahedral chloro complexes of the type $[FeCl_x(H_2O)_{6-x}]$ are coexisting with $[FeCl_4]^-$ in DP. Another point that we noted in the analysis of the Fe K-edge EXAFS of DP, is that no peak attributable to Fe–Fe could be found in the Fourier transform (see Fig. 9). Thus the dimeric species Fe_2Cl_6 is unlikely to exist, at least as one of the main solute species, in DP and in a concentrated solution of $FeCl_3$.

TABLE 3. RESULTS OF THE CURVE-FITTING ANALYSIS OF THE EXAFS DATA OF $FeCl_3$ SOLUTIONS

Solution	Coordination number		Distance (r/Å)		S*
	Cl	O	Fe-Cl	Fe-O	
0.1N	0.8	5.2	2.35 (4)	1.99 (2)	0.50
0.7N	0.8	5.2	2.28 (3)	2.00 (2)	0.40
3N	2.0	4.0	2.30 (3)	2.02 (2)	0.42
4N	1.8	4.2	2.30 (3)	2.02 (2)	0.60
0.5A	0.8	5.2	2.26 (3)	1.98 (2)	0.52
3A	2.0	4.0	2.30 (3)	2.01 (2)	0.60
Cl3A	2.0	4.0	2.30 (3)	2.04 (2)	0.50
DP	3.0	2.0	2.22 (2)	1.93 (4)	0.40

* The inaccuracy of these S values was found to be 20—30%.

Discussion

Summarizing the experimental results concerned with Fe K-edge EXAFS and XANES together with those of UV-visible absorption spectroscopy, we can derive the following conclusion for the solute state in the $FeCl_3$ aqueous solution. In the solutions of $FeCl_3$ concentration of 0.1—1 mol dm^{-3}, the solute is mainly in the state of $[Fe(H_2O)_6]^{3+}$ but partially in the state of other complexes, such as $[FeCl(H_2O)_5]^{2+}$. The average Cl coordination number increases with the increase of $FeCl_3$ concentration, and $[FeCl_2(H_2O)_4]^+$ becomes the main solute species in the solutions of the concentration of 3—4 mol dm^{-3}. Although the coexistence of $[FeCl_4]^-$ is expected from the results of UV-visible absorption spectroscopy, its amount is likely to be very small as far as we judge from the results of X-ray absorption spectroscopy. In the discussion given in the present paper, we have not explicitly taken up the hydrolysis products of the type $[FeCl_x(H_2O)_{6-x-y}(OH)_y]$ derivable from $[FeCl_x(H_2O)_{6-x}]$, which are reported to be formed in a non-acidified solution. Unfortunately, it is hard to distinguish the formers from the latters in the analysis of the EXAFS data. Therefore, whenever we say $[FeCl_x(H_2O)_{6-x}]$, it should be taken to include also the corresponding hydrolysis products.

Magini and Radnai considered that the main species in the solution of $FeCl_3$ concentration of about 4 mol dm^{-3} is $[FeCl_3(H_2O)_3]$.5) But this kind of octahedral chloro complex has never been found among the crystals of iron(III) compounds, and the results of the present study have shown that the solute mainly exists in the state of $[FeCl_2(H_2O)_4]^+$ in the solution of the $FeCl_3$ concentration of 3—4 mol dm^{-3}, in disagreement with the conclusion by Magini and Radnai. There seems to be no indication for the existence of $[FeCl_3(H_2O)_3]$. Seemingly in an aqueous solution of $FeCl_3$, an octahedral complex becomes less stable than a tetrahedral complex as the Cl coordination number exceeds 2 probably because of the increase of the repulsive cis-cis interaction between Cl^- ions.

In the case of DP, the EXAFS data indicate that the solute is partly in the state of $[FeCl_4]^-$ and partly in the state of the octahedral chloro complexes. We estimated the fraction of $[FeCl_4]^-$ to be about 50% from the height of the pre-edge peak associated with 1s-3d transition. The remaining part is most likely to be in the state of $[FeCl_2(H_2O)_4]^+$. The Cl/Fe ratio derived from the analysis of the EXAFS data can be satisfactorily understood with this model. From the present study of XANES and UV-visible absorption spectra we can conclude that $[FeCl_4]^-$ starts to be formed at the $FeCl_3$ concentration of about 4 mol dm^{-3}, though the amount may not be so large at this concentration. Inoue *et al.* reported that the physical properties of the $FeCl_3$ aqueous solution abruptly change at the $FeCl_3$ concentration of about 4 mol dm^{-3}, and attributed this behavior to the formation of $[FeCl_4]^-$.30) This is consistent with our conclusions.

It has been often assumed that the $FeCl_3$ dimer, Fe_2Cl_6, is formed in a concentrated $FeCl_3$ solution.5,6,8) However, no peak corresponding to Fe–Fe distance of Fe_2Cl_6, which is reported to be 2.75—2.80 Å by Magini,6) can be found in the Fourier transform of the EXAFS data of DP. Thus we conclude that Fe_2Cl_6 is unlikely to exist, at least as one of the dominant species, in a concentrated $FeCl_3$ solution.

The authours are grateful to Dr. T. Matsushita and Dr. H. Oyanagi for their helpful advice for the XAS measurement at the Photon Factory. The authors also thank to Dr. I. Ikemoto and Dr. N. Kosugi for their discussions and helps in the XAS experiments.

References

1) G. W. Brady, *J. Chem. Phys.*, **29**, 1371 (1958).

2) G. L. Standley and R. F. Kruh, *J. Chem. Phys.*, **34**, 1450 (1961).

3) G. W. Brady, M. B. Robin, and J. Varimbi, *Inorg. Chem.*, **3**, 1168 (1964).

4) M. D. Lind, *J. Chem. Phys.*, **46**, 2010 (1967).

5) M. Magini and T. Radnai, *J. Chem. Phys.*, **71**, 4255 (1979).

6) M. Magini, *J. Chem. Phys.*, **76**, 1111 (1982).

7) D. L. Wertz and M. L. Steele, *Inorg. Chem.*, **19**, 1652 (1980).

8) D. L. Wertz and M. D. Luter, *Inorg. Chem.*, **20**, 3118 (1981).

9) M. D. Luter and D. L. Wertz, *J. Phys. Chem.*, **85**, 3542 (1981).

10)G. Giubilo, M. Magini, G. Lichen, G. Pashina, G. Piccaluga, and G. Pinna, *Inorg. Chem.*, **22**, 1001 (1983).

11) "EXAFS Spectroscopy," ed by B. K. Teo and J. C. Joy, Plenum Press (1981).

12) M. Nomura, K. Asakura, U. Kaminaga, T.Mastushita, K. Kohra, and H. Kuroda, *Bull. Chem. Soc. Jpn.*, **55**, 3911 (1982).

13) H. Kuroda, I. Ikemoto, K. Asakura, H. Ishii, H. Shirakawa, T. Kobayashi, H. Oyanagi, and T. Mastushita, *Solid. State. Commun.*, **46**, 235 (1983).

14) M. Nomura, D. Sci. Thesis, The University of Tokyo, Tokyo, Japan, 1982.

15) H. Oyanagi, T. Matsushita, M. Ito, and H. Kuroda, *KEK Report* 83/30 (1984).

16) E. Rabinowitch and W. H. Stockmayer, *J. Am. Chem. Soc.*, **64**, 335 (1942).

17) H. L. Friedman, *J. Am. Chem. Soc.*, **74**, 5 (1952).

18) G. A. Gamlem and D. O. Jordan, *J. Chem Soc.*, **1953**, 1435.

19) S. Balt, *Mol. Phys.*, **14**, 233 (1968).

20) L. N. Mulay and P. W. Selwood, *J. Am. Chem. Soc.*, **76**, 6207 (1954).

21) The height of the pre-edge peak observed in the spectra of $[FeCl_4]^-$ and $[FeCl_2(H_2O)_4]^+$ were used for the evaluation of the amount of $[FeCl_4]^-$ from the spectrum of DP.

22) "International Tables for X-ray Crystallography," ed by C. H. Macgillavry, G. D. Rieck, and K. Lonsdale, Kynoch Press (1962).

23) The relative positions of the points in this plot were not affected by changing the E_0 value or by extending the k range of the EXAFS data used in Fourier transformation. No essential change was resulted even if we took the Fourier transform of $k \cdot \chi(k)$ instead of that of $k^3 \cdot \chi(k)$.

24) B. K. Teo, M. R. Antonio, and B. A. Averill, *J. Am. Chem. Soc.,* **105**, 3751 (1983).

25) B. K. Teo, P. A. Lee, A. L. Simons, P. Eisenberger, and B. M. Kincaid, *J. Am. Chem. Soc.,* **99**, 3854 (1977); P. A. Lee, B. K. Teo, and A. L. Simons, *ibid,* **99**, 3856 (1977).

26) From the study of the reference samples, the S value was concluded to be about 0.5 both for Cl and O.

27) M. D. Lind, *J. Chem. Phys.,* **47**, 990 (1967).

28) A. Ferrari, L. Cavalca, and M. Tani, *Gazz. Chim. Ital.,* **87**, 22 (1957).

29) M. D. Lind, *Acta. Crystallogr., Sect. B,* **26**, 1058 (1970).

30) Y. Inoue, S. Seki, M. Yokoyama, N. Masaie, and Y. Kanaji, *Nippon Kagaku Kaishi,* **1974**, 2297.

31) N. J. Hair and J. K. Beattie, *Inorg. Chem.,* **16**, 245 (1977).

32) B. Zaslow and R. E. Rundle, *J. Phys. Chem.,* **61**, 490 (1957).

33) B. N. Figgis, C. L. Taston, R. P. Sharme, and A. H. White, *Aust. J. Chem.,* **31**, 2717 (1976).

34) J. K. Bearrje and C. J. Moore, *Inorg. Chem.,* **21**, 1292 (1982).